Prediction of Tribological Behavior of Candidate Materials for Rotor Seals

A Senior Project

Presented to

the Faculty of the Materials Engineering Department

California Polytechnic State University, San Luis Obispo

In Partial Fulfilment

of the Requirements for the Degree

Bachelor of Science

By

John Franzino & Will Michul

June, 2014

Approval Page

Project Title: Prediction of Tribological Behavior of Candidate Materials for Rotor Seals

Author: John Franzino & Will Michul

Date Submitted: June 9, 2014

CAL POLY STATE UNIVERSITY
Materials Engineering Department

Since this project is a result of a class assignment, it has been graded and accepted as fulfillment of the course requirements. Acceptance does not imply technical accuracy or reliability. Any use of the information in this report, including numerical data, is done at the risk of the user. These risks may include catastrophic failure of the device or infringement of patent or copyright laws. The students, faculty, and staff of Cal Poly State University, San Luis Obispo cannot be held liable for any misuse of the project.

Prof. Trevor Harding
Faculty Advisor

_____
Signature

Prof. Katherine Chen
Department Chair

_____
Signature

Abstract

To reduce high costs associated with manufacturing and testing materials for rotor seals, a procedure needs to be developed to quickly and accurately test candidate materials as they are released. The test should reduce the amount of fabrication required and model working conditions in order to accurately assess the tribological behavior of candidate materials. A possible solution was examined that utilized a rig meant to model operational stresses and wear. Compression modulus data was then taken in order to quantify the accumulation of damage due to microcracking, the primary mode of failure, through a damage index parameter. Testing results concluded that the methods used do not recreate working conditions accurately enough to obtain reliable tribological data due to high variability in the rig, the introduction of damage not typically seen in working rotor seals, and only one failure mode is being accounted for.

Keywords: tribological, rotor seal, fatigue, microcrack, accumulation of damage, damage index

List of Tables

List of Figures

Acknowledgements

We would like to thank our advisor, Dr. Trevor Harding, for his guidance and support throughout the course of the project; IDEX Health and Science and our contacts Jon Nichols and Alexei Abras for the opportunity to work on this project, their input and guidance, and financial and material support; Dr. Joseph Mello and Deep Shah for their help in the Mechanical Engineering Composites Lab. Finally, we would like to thank Dr. Blair London for his help with the use of testing equipment.

Table of Contents

Introduction

Overview

One of the main products of IDEX Health and Sciences under the brand Rheodyne is a multi-position injector assembly which is used primarily in high pressure liquid chromatography (HPLC), an analytical chemistry process used to identify and quantify the components in a given solution (Figure 1). Within the assembly itself, a high pressure, liquid-tight seal is achieved by pressing a rotor seal against a stator surface. This project focuses on developing a multi-phase materials selection procedure for candidate rotor seal materials based on functional requirements of the application and known failure phenomena of currently used materials.

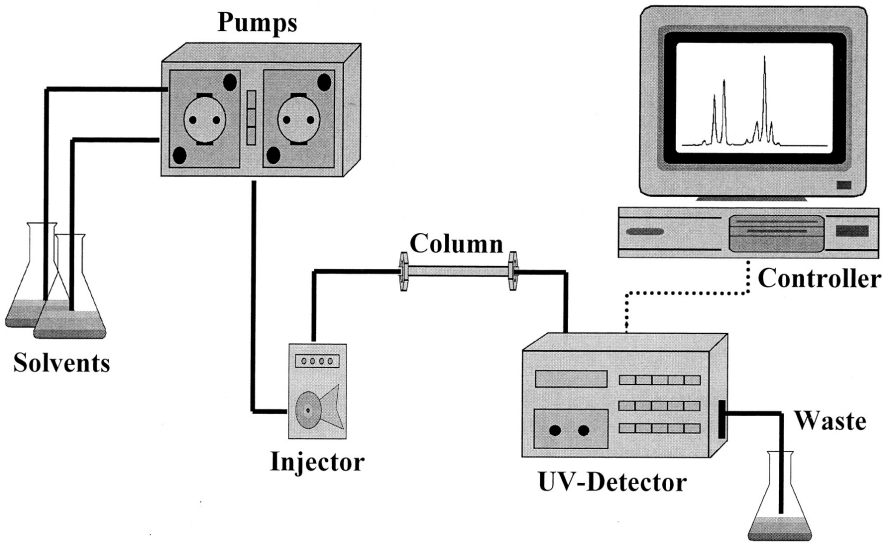

Figure 1: HPLC process and equipment assembly. The rotor seal is located in the injector assembly.

The rotary shear valve developed by IDEX Health and Sciences is a polymer seal for a multi-position selector valve assembly (Figure 2). It is designed to seal the valve ports and control which ports are open at specific points in the chromatography process. Through a process of pressurization and passing a sample through a sorbent material packed in a column, the components of the sample can be identified and quantified based on the time each component takes to pass through the sorbent.[1]

Figure 2: A multi-position valve assembly produced by IDEX. The input ports can be seen on the right end of the assembly with a volumetric holding loop attached.

The seal is a cylindrical puck with a diameter of 0.6250 in and a thickness of 0.1250 in. A series of grooves are machined into the surface which is in contact with the stator surface. These grooves act as channels to select which input ports are open for loading, pressurization, or discharging as dictated by the given HPLC procedure. The default configuration for the channel design has three channels with radial arcs of 80°. Separating each channel is a land, or unmachined section of the seal. This land is key in maintaining the sealed pressure differentials between the channels during operation. Depending on the desired procedure and application, the customer may request specially designed channel configurations, or a standard configuration is used (Figure 3).

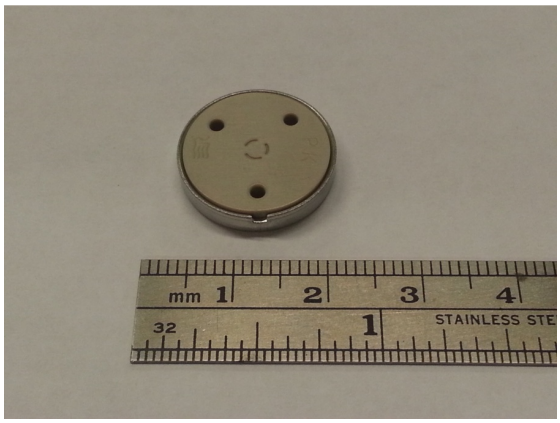

Figure 3: A standard polymer rotor seal with the machined switching channels shown.

When the chromatography process is started, high pressures (10-20 ksi) are applied to the seal, pressing it against the stator surface. When in the loading position, the channels allow the sample to enter the volumetric loop attached to the valve assembly and be held there. Once the loop is filled, the seal rotates so that the channels are positioned to open the loop to the separating column. Because of the extremely high pressure difference between the sample and the separating column, the sample is injected at high speeds through the column. This high speed allows for the time taken by each component of the sample to pass through the column to be used to determine the composition of the sample.

In addition to the high compressive force needed to create a liquid-tight seal, the rotor seal is also rotated to adjust which ports are opened or closed; this motion introduces a shear stress component. The rotation can range based on the procedure being used, but the default channel design is set at 60 degrees, and can range from rotation times of 100ms to 1s. The shear stress created by this rotation is crucial as it puts the rotor seal in dynamic contact with its counter-surface. Because of the cyclic nature of the movement, the seal experiences fatigue loading. Whenever fatigue loading or dynamic contact between two materials is present within a system, components of that system are going to have a finite service life. For the working conditions presented, IDEX expects the seals to have a life of 60,000 movements.

Functional Requirements

To prevent degradation of the material due to reactions with chemicals, seal materials must have high chemical resistance. Because of the applications of HPLC can range from medical research to industrial uses, there is a wide range of substances (with a wide range of pH values) that the seal can be exposed to. The main threats for degradation are organic solvents; these solvents are used to dissolve the analytes of the sample, and will be present in nearly all samples. With this in mind, the seal must remain inert in the presence of these organic solvents in order to maintain a functional liquid-tight seal during operation. Common chemicals include acetone, methanol, acetonitrile, chloroform, hexanes, anhydrous ether, and methylene chloride.

The seal also must be able to withstand high compressive loads during operation, typically ranging between 10-20 ksi. Not only must the polymer puck withstand the loads, but the machined channels must maintain their geometry so that the valve will operate as designed and prevent leaks. The machining of the channels on the seal surface adds a considerable stress

concentration factor due to the geometry. Therefore the compression strength properties of a completed seal must be high enough so that the machined channels will not collapse during operation. In order to pass a candidate material given this criteria, baseline property values can be determined from rotor seal materials which are currently in production and use in HPLCs. As these materials are currently in use for rotor seals, it is known that their compression strength values will maintain the final part geometry under working conditions, so any materials with properties below these values should be rejected.

As a result of the seal being rotated in order to change which ports are opened and closed during the HPLC process, the rotor seal is in dynamic contact with the counter-surface. This motion induces both wear and fatigue loading. For this reasoning, it is imperative that the triobological properties of the seal and its counter surface are optimized to increase the service life of the seal. Currently, IDEX has set the minimum acceptable service life at 60,000 cycles. Therefore, all candidate materials must meet or exceed the currently used materials in terms of their service life, and subsequently must have better trioblogical properties.

Current Seal Materials

Polyether ether ketone (PEEK) is a semi-crystalline thermoplastic that exhibits high strength mechanical properties while being resistant to chemical and fatigue inducing environments while having good thermal stability. PEEK is an excellent material for a large array of thermomechanical applications due to its ability to retain flexural and tensile properties at very high temperatures (250°C). Although PEEK has a high resistance to attack by many organic solvents, it has poor resistance against some acids because it is synthesized through step-growth polymerization which uses polar aprotic solvents containing acidic hydrogen. PEEK also exhibits one of the lowest outgassing rates of any thermoplastic, which is why it is used in vacuum applications.[2]

The thermal stability of PEEK is a property of the linear aromatic backbone which is extremely stable and makes up the bulk of the monomer (Figure 4). In the case of all polymers, pyrolysis begins at the weakest link. In the case of PEEK, the ratio of these weak links (bridging groups between aromatic units) to the number of aromatic units per monomer is low.[3] The strong linear aromatic backbone that gives PEEK its thermal stability is the same reason that PEEK exhibits high chemical resistance.[3]

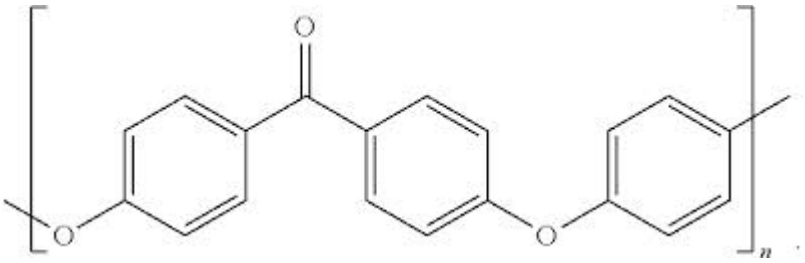

Figure 4: Chemical structure of a PEEK monomer.[3]

In polymers, one dictating factor in determining strength is the degree of crystallinity. As more of the polymer chains align in crystalline regions as opposed to an amorphous arrangement, the strength of the polymer increases. For PEEK, crystallinity can reach 48%, providing a more rigid material than other thermoplastics.[3] With the addition of filler materials that can include chopped fibers or carbide particles, the strength of the polymer is greatly increased, allowing it to withstand the pressures experienced during HPLC. IDEX currently uses several proprietary PEEK-based polymer blends and composites.

Polyimides are a subset of thermosets. Similar to PEEK, commonly used polyimides consist of an aromatic backbone structure. The aromatic backbone results in similar chemical resistance to most common solvents and lubricants, and thermal stability similar to PEEK. Polyimide strength also arises from the higher crystallinity of the polymer and the crosslinking between polymer chains that occurs during the thermoset process.[4,5] Because polyimides exhibit many properties similar to advanced PEEK blends which are well suited for the application, IDEX is considering several polyimides. There are many subsets of polyimides, though at this time the specific types being considered by IDEX are not known as IDEX is currently working on a basis of coded material names.

Current Problem

Due to the finite service life of the rotor seal, new materials are always being sought out to extend this life time; however, the current testing procedure is both time and money intensive (Figure 5). After a sales representative from a compounding company, or an employee at IDEX, identifies a new candidate material, the minimum purchase order of 10kg of the new blend must be obtained. IDEX approximates this cost at about $2,500 per material. In addition to the cost

associated with acquiring the new blend, the blend also needs to be manufactured into the puck geometry. Currently IDEX spends about $1,500 to injection mold 300 pucks; however this cost varies because the pucks are sometimes extruded. Following the main manufacturing step, the newly formed pucks must be fabricated into rotor seals. This includes machining the intricate switching channels, as well as the final finishing steps. In total, the cost associated with transforming the pucks into finished rotor seals is estimated to be $800. Once the final part is ready, 12 rotor seals are used in the assembly of 12 new valves which are used for the life cycle test. Each one of the new valves costs $225 to assemble, not including the cost associated with the new rotor seals, and at the end of the life cycle test the valves have no value. Unfortunately, upon completion of the life cycle test, the vast majority of tested materials are rejected because they do not perform better than currently used materials. A rejection at this step in the testing procedure results in about $7,500 and months in potential production time wasted.

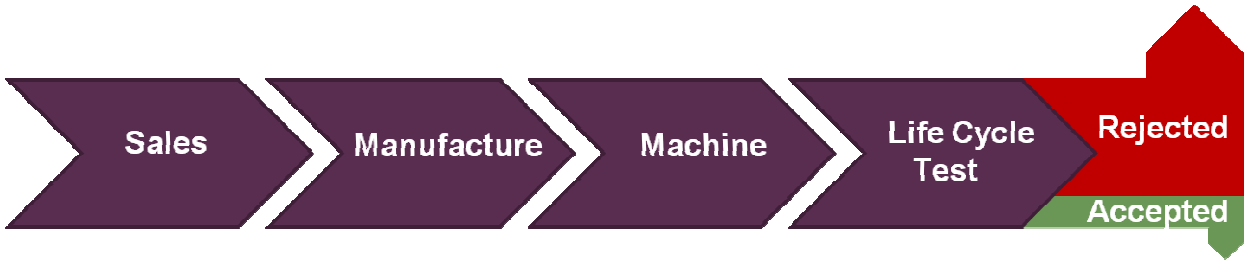

Figure 5: Process flow diagram of the current life-cycle testing procedure.

Problem Statement

Currently, all candidate materials for rotor seals, as identified by the compounder and IDEX, undergo the full manufacturing and life-cycle testing procedure. However, as with all research and development, the success rate for finding better materials is very low. As a result of this low success rate, much time and money is spent on the manufacturing and testing of materials that do not prove successful. A preliminary testing procedure must be developed in order to reduce the amount of time and money wasted in the R&D process by rejecting poor material choices before they are manufactured and life-cycle tested. This preliminary testing procedure needs to address the pass/fail functional requirements of being chemically resistant to a wide range of organic solvents and have enough compressive strength to up hold the groove geometry, while also quantitatively and qualitatively evaluating the tribological performance of the candidate materials.

Justification of Problem Statement

By implementing a preliminary screening step in the full life-cycle procedure, the majority of rejections can be made on the front end of the full procedure, subsequently increasing the acceptance rate on the back-end of the full life-cycle procedure (Figure 6). Comparatively, a rejection at the preliminary screening processes has much less embodied time and money than a rejection at the end of life-cycle testing—about $4,500 and $7,500, respectively

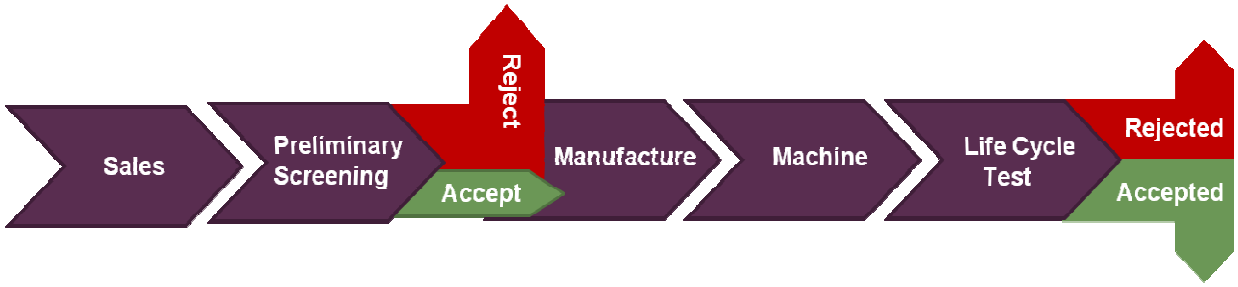

Figure 6: Process flow diagram of the proposed life-cycle testing procedure.

Failure Analysis

Before candidate materials can be examined, a failure analysis was needed in order to fully understand the failure mechanics of currently used materials for rotor seals under working conditions. IDEX provided several samples of the three currently used materials, Polymer A, Polymer B, and Polymer C, as well as two materials that failed immediately during life cycle testing, PEEK A and PEEK B. These sample rotor seals have already undergone lifecycle testing at the IDEX facility. By examining these failed rotor seals, the primary modes of failure can be identified so that a possible screening test can be developed that aimed to test or quantify the properties that are tied to them. Each sample was imaged using a FEI Quanta 200 scanning electron microscope (SEM) set in low-vac mode with a voltage of 3.5 kV, a spot size of 4, and a pressure of 60-80 Pa. This imaging technique allows for the capture of clear images of non-conductive materials with a depth of field which highlights surface features. A stereo optical microscope was also used in order to a macro view of the damage on the rotor seals.

Adhesive Wear

Under high pressure operating conditions, the seal has been shown to adhere to the stator DLC surface, leaving seal material on the stator when separated. In this failure mode, asperities

from the opposing surfaces become atomically bonded due to the few asperities in contact bearing the vast majority of the mechanical load over a very small area, therefore experiencing huge compressive stresses. As the two surfaces continue to move in respect to one another, the shear stress increases until the shear strength of the polymer is reached and ruptures along the shear plane. The polymer asperity is now detached from the polymer surface and can adhere to the DLC surface (Figure 7). This adhesion could be a compounding factor in spalling or wear failure. As the seal adheres to the stator and continues to be rotated, it would add a new source of complex stresses which could increase fatigue rate. Adhered polymer particles could also break free, causing another source of abrasive wear. This then has the potential to create a wear track as the seal is rotated, eventually creating grooves that would bridge the land between two channels. The regions identified as adhesive wear on the samples provided by IDEX showed a lack of failure characteristics other than large smooth areas where it looked like a section of the material was lifted away, as seen in Figure 8.

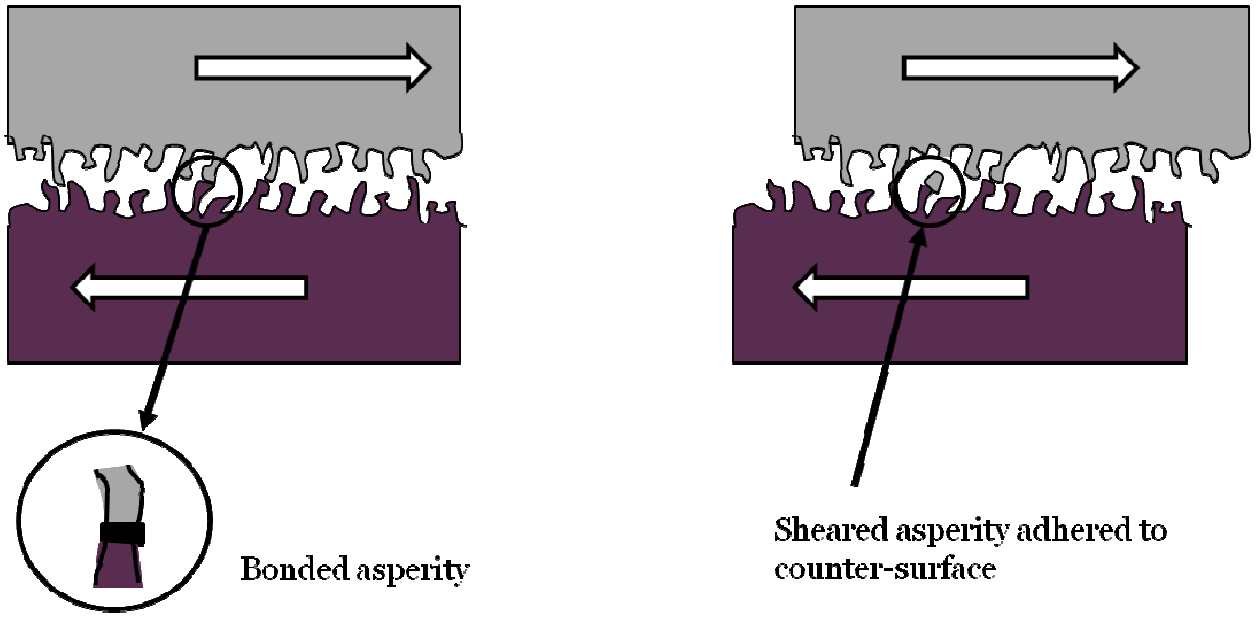

Figure 7: Schematic depicting the phenomenon of adhesive wear.

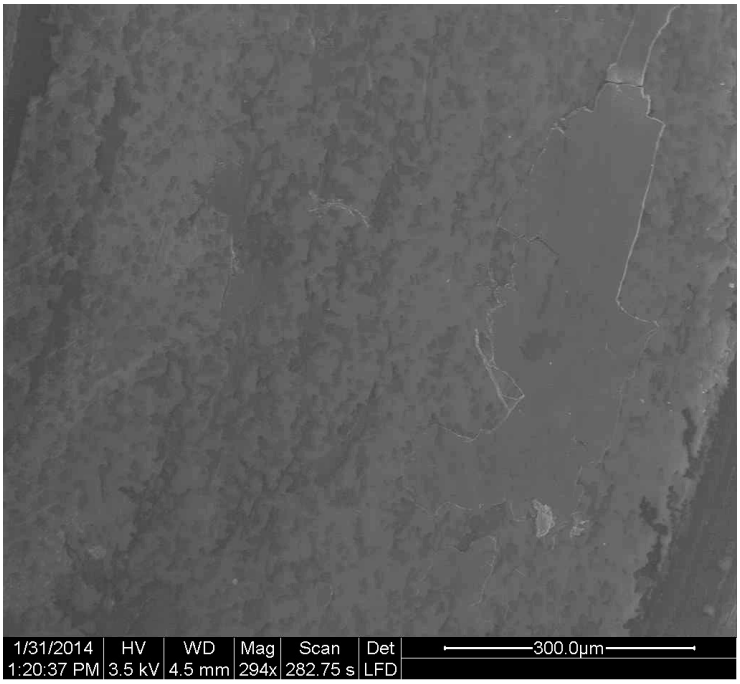

Figure 8: Adhesive wear area on sample Polymer B-1. A lack of divots, gouges, scratches, or cracking indicates plastic on plastic wear. The large smooth area on the right of the image was a feature seen throughout the adhesive wear areas on both samples.

Microcracking

The most dominant mode of failure seen in the analyzed samples is microcracking, as it is seen in all of the sample materials except one. The mechanisms of surface and subsurface fatigue occur when a sliding motion creates an alternating force or stress oriented in a direction normal to the surface. The combination of the compression and shear stresses placed on the rotor seal initiates the formation of cracks slightly beneath and parallel to the surface which then propagates suddenly toward the surface, causing pits to form as particles of the material are ejected or worn away, a phenomenon called spalling. Spalls are characterized by the presence of flat-bottomed pits with steep walls seen on failed seals (Figures 9 and 10). This failure mechanism creates leak paths between the machined channels and a resulting failed rotor seal, as seen in Figures 11 and 12.

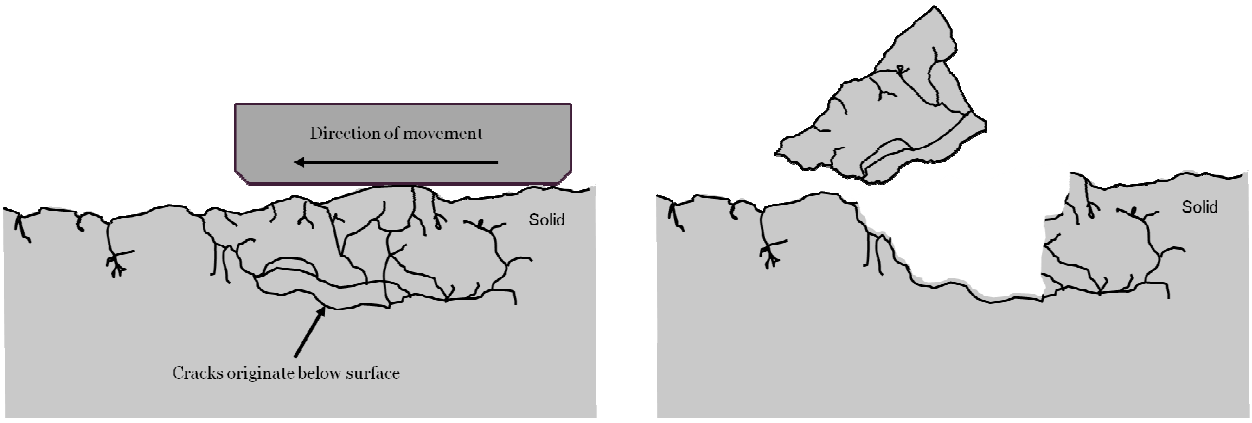

Figure 9: Schematic depicting microcracking due to two surfaces in dynamic contact that results in a spall.

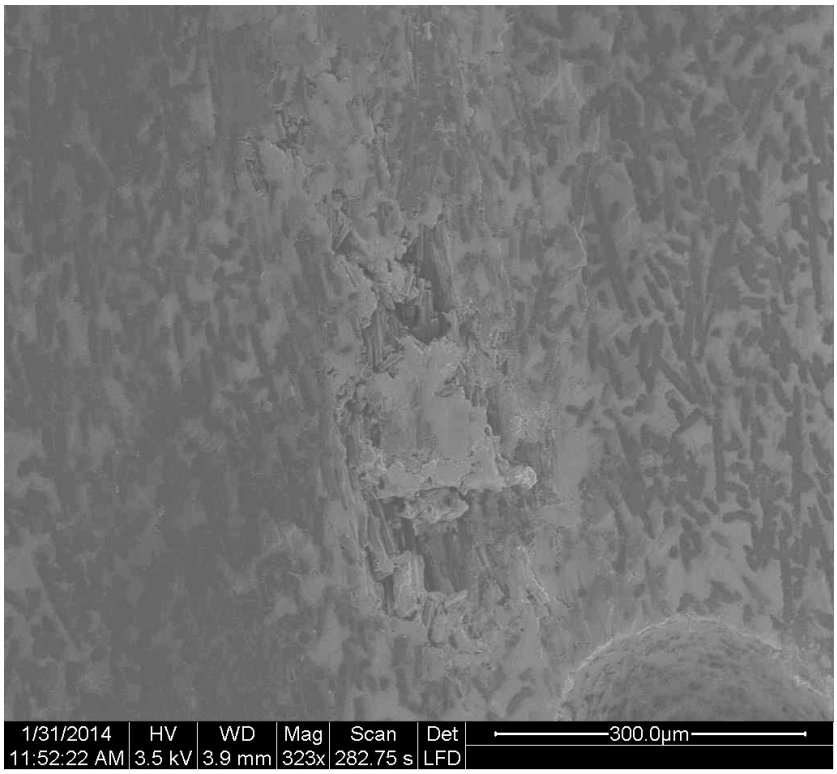

Figure 10: Divot on a land on sample Polymer C-2. The flat bottom and steep walls are characteristic of spalling failure. Fibers are visible protruding from all surfaces of the divot.

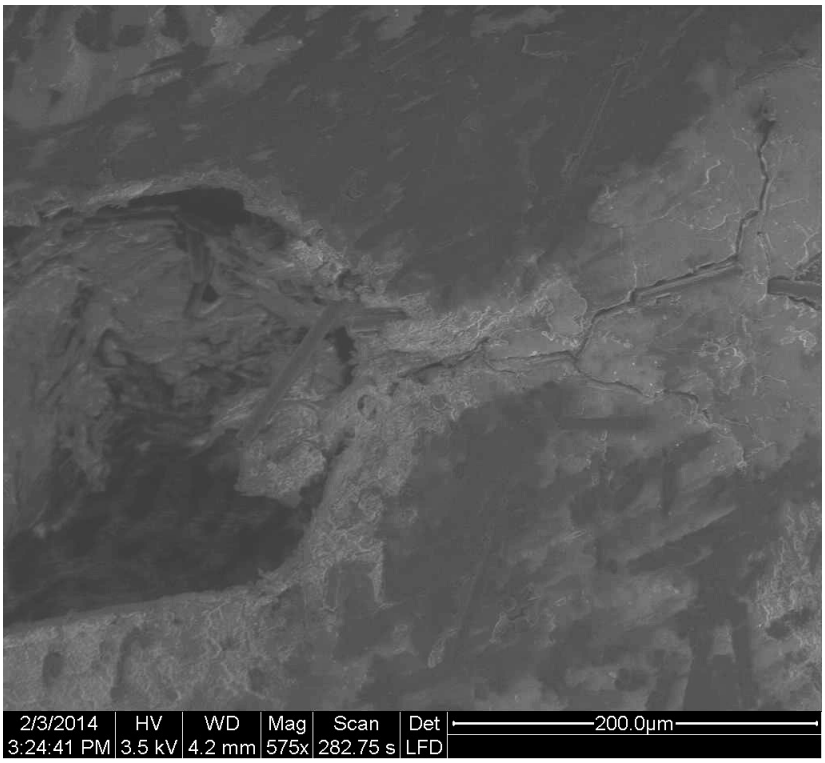

Figure 11: Microcracking on a land on sample Polymer A-1. Fibers are visible along the axis of the cracks.

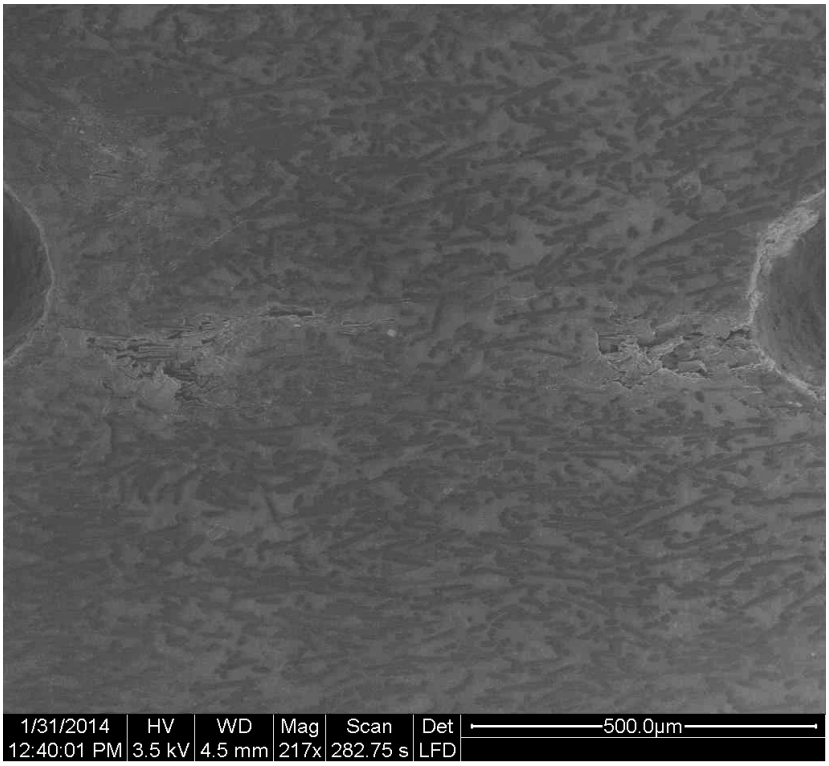

Figure 12: Microcracking and resulting spalling divots on a land for sample Polymer C-1.

This form of fatigue is common in applications where an object repeatedly rolls across the surface of a material resulting in a high concentration of stress at each point along the surface. The amount of surface and subsurface fatigue is directly correlated to the stress concentration factor which dictate the nucleation and propagation rate of microcracks until they reach a critical crack size.[6]

in all of the materials with the known presence of fiber reinforcement, the formation of microcracks and spalling divots also occurs. This is highlighted in Table I, which shows the presence of the various failure modes and characteristics of the rotor seals. In the table, an "x" indicates the presence of that category, a mark of "~" indicates a suspected but not confirmed presence, and no mark represents an absence of that failure mode on the sample.

Table 1: Failure modes present in samples.

Sample Material	S/N	Divots/Spalling	Adhesive wear	Fiber Reinforcement	Microcracking
PEEK A	1	x		x	x
PEEK A	2	x		x	x
PEEK B	1	x		x	x
PEEK B	2	x		x	x
Polymer A	1	x	~	x	x
Polymer A	2	x		x	x
Polymer A	3	x		x	x
Polymer B	1		x		
Polymer B	2		x		
Polymer C	1	x	~	x	x
Polymer C	2	x		x	x

All of the samples that have fibers exhibit microcracking and spalling. Alternately, the only sample which does not exhibit these failure characteristics was Polymer B, which does not have any reinforcement fibers. However, it does exclusively show adhesive wear, with the only other cases only being suspected on one sample of Polymer C and one Polymer A.

When the material is loaded under working conditions, the interface between the matrix and fibers is acting to transfer the load to the stronger fibers, so it is a main area for failures that start with a debonding of the two materials which provides an ideal site for microcracks to nucleate (Figure 13).[7] This debonding is a result of the difference in strength between the fibers and the interface with the surrounding polymer matrix.[7] It should be noted that these microcracks in these sample are so far along in the propagation phase that they have reached the surface of the material and are visible on a relatively macroscopic level, resulting in the critical leak rates that lead to part failure.

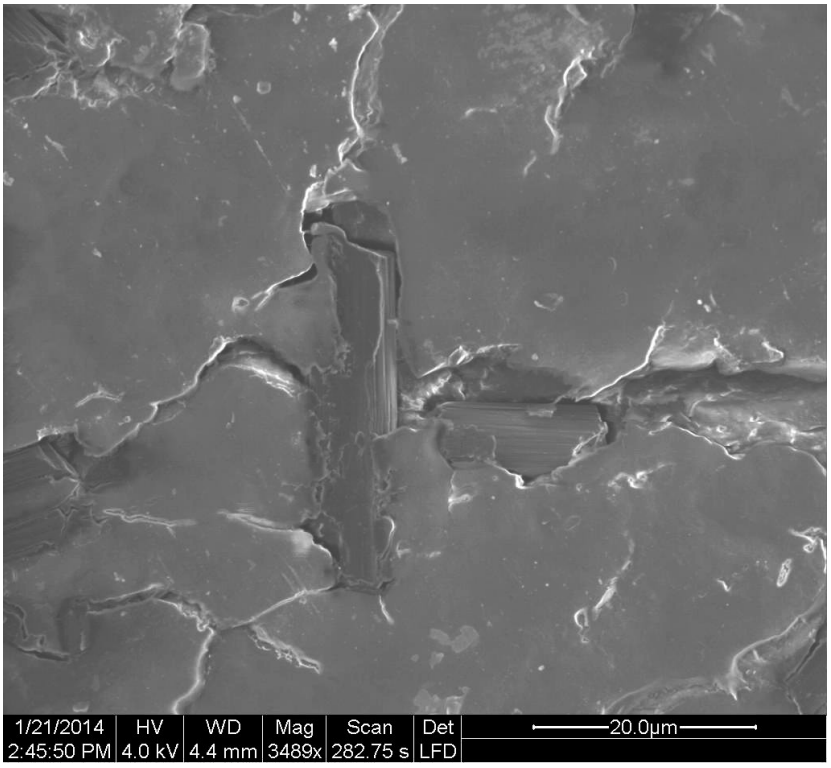

Figure 13: High magnification image of cracks occurring at the interface between the polymer matrix and the reinforcement fibers of Polymer A-2.

Polymer B may be the only material to experience adhesive wear because it does not have the reinforcement fibers as seen in the other materials, so it is able to endure cyclic testing without the formation of microcracks. Because microcracks did not form and fail the rotor seal,

the failure mode of adhesive wear was able to manifest much earlier than it might have in materials with fiber reinforcement.

Abrasive Wear

Whenever two materials are in dynamic contact, abrasive wear will occur. The loss of material resulting from abrasive wear is due to hard particles or asperities being forced past each other. This failure mode is further amplified when the two materials in question are dissimilar. In this system, a polymer rotor seal is rubbing against a metal stator surface with a diamond like coating (DLC). As a result, the difference in hardness between the two surfaces is high; therefore the likelihood of an asperity on the polymer surface becoming dislodged is increased.

Reinforcing particles, like carbides or fibers, in the polymer can also act as abrasives if they break out as a result of spalling or wear from friction. Because these reinforcing particles are made from materials with extremely high hardness, they are very effective at behaving as abrasive debris. The stator's DLC can also contribute abrasive particles when it breaks off at weak points on port corners due to higher stress concentrations and the presence of a thinner coating. Loose DLC particles then act as abrasives and increase wear rate. When particles from either surface are freed, a positive feedback loop is formed, as the freed particles create more particles, and the wear rate increases. As the seal and stator are degraded, the lands and precise edges of the channels and ports are eliminated, creating leaks which render the seal ineffective.

Failure Analysis Conclusions

With the findings of this analysis, it was concluded that the main mode of failure for the rotor seal was microcracking. Because all materials except Polymer B exhibited microcracking to some degree, any materials that are to be examined in the future should take into account the propensity to form microcracks. For this reason, the failure mechanic of microcracking is the focus of this study. Even though Polymer B did not form microcracks, this can be attributed to the absence of reinforcing fibers, whose interface with the polymer matrix was shown to be a failure zone as a result of debonding. The adhesive wear that Polymer B did exhibit is a failure mode to consider, but because it is believed to occur at a level of use beyond that which microcracking damage occurs at, it can be considered secondary until the mechanics of microcracking are understood and can be tested for. Similarly, while abrasive wear is a

significant cause for concern, it is primarily a result of the other main modes of failure like microcracking, so it can also be considered a secondary concern for this study.

Qualification Testing

Development of Testing Procedure

Unacceptable valve performance is the result of micro-fluidic leak pathways created by voids in the material. The voids are most often the result of the micro-cracks which nucleate at the fiber-matrix interface, eventually accumulating and propagating to a critical density and size that either causes a surface spall or simply creates a large enough crack for high pressure liquid to travel through. Because microcracking is identified as the primary mode of failure, a testing procedure which quantifies this mode of failure is most desired. It is important to note that by focusing on quantifying one mode of failure all other failure modes are effectively ignored. However, due to the complex nature of tribological properties, incorporating all failure modes in one test is not realistic for this study.

Microcracks are one type of void found within a fatigued material; voids, in turn, reduce the stiffness of a material by providing a resistance free path for elastic deformation. Therefore by monitoring the change in elastic modulus of a sample, on a per cycle basis, the accumulation of damage can be quantified by:

$$D_N = 1 - \frac{E_N}{E_0} \qquad \text{(Eq. 1)}^{8}$$

in which E_N is modulus at cycle number N and E_0 is the initial modulus (N=1). The damage index D was be calculated for each cycle (N=1→ N=250) and then be plotted in respect to N.[8]

Materials & Methods

In order to quantify a materials resistance to the accumulation of micro-cracks a simple compression-compression fatigue test was conducted on a servo-hydraulic Instron. To determine if the damage index is a valid way to measure the accumulation of microcracks, the preliminary test will be conducted on two distinct samples. While the two samples were the same material,

polymer A, one sample was undamaged while the other had been previously ran until failure in IDEX's life cycle tester.

While inducing a compressive stress of 15 ksi on polymer pucks, the strain of the sample was measured using a strain gauge (Vishay Micro Measurement EA-09-031EC-120) was adhered to the outer diameter of each puck, in accordance with Vishay's sample preparation techniques for M-Bond 200 adhesive. Using the outputted stress and strain data, the elastic modulus was calculated on a per cycle basis; the corresponding damage indices were then calculated (see Appendix A for details).The tests were run to a total of 250 cycles, at a frequency of 1 Hz. This procedure was conducted in accordance with ASTM standards D0695-10 and D7791-12, when applicable.[9,10]

Results & Discussion

Upon comparing the damage index for the damaged and undamaged Polymer A samples, it is evident that the rate of damage accumulation is greatly different (Figure 14). Since the damaged sample was examined in the failure analysis, it can be said with certainty that an abundance of microcracks are present within the sample. This is contrasted with the undamaged sample in which no microcracking is present.

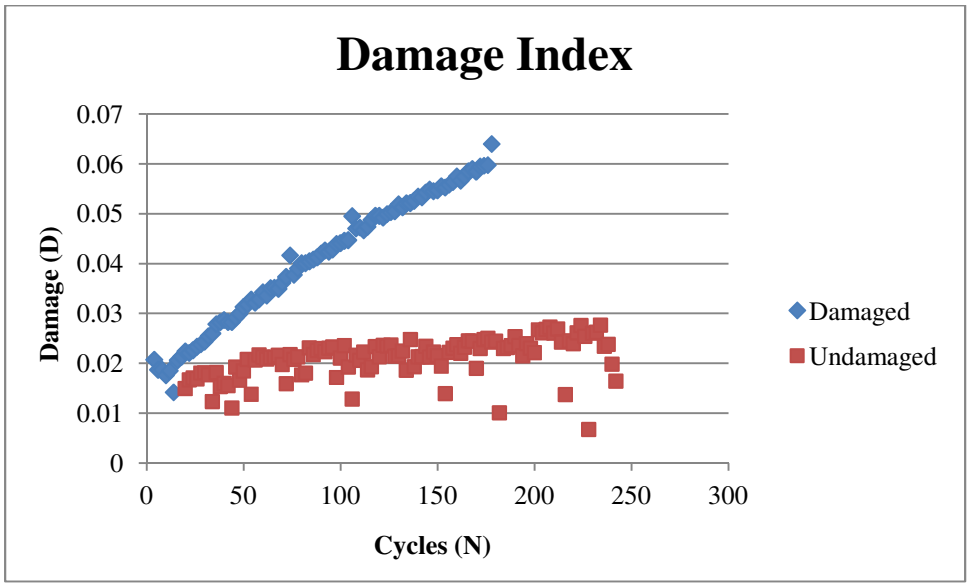

Figure 14: Damage index of a damaged sample compared to an undamaged sample.

The steep slope of the damage index for the damaged sample is characteristic of a stiff, reinforced polymer in the final phase of fatigue failure. In this final stage, microcracks have already propagated to a relatively macroscopic size; it is the propagation of these macroscopic cracks, along with fiber fracture, which results in the high rate of damage accumulation.[8]

Interestingly, the slope of the damage index for the undamaged sample is not characteristic of a stiff, reinforced polymer in the initial phase of fatigue failure. Typically, as fatigue failure initiates, the rate of damage accumulation is high—about the same as seen as in the final phase of fatigue failure. The high initial stiffness reduction typically seen during fatigue failure is attributed the nucleation of microcracks and voids.[8] Nucleation happens so readily during this initial phase due to the presence of fiber reinforcements which effectively act as defects within the polymer matrix due to the large difference in stiffness of the two materials. However, a high rate of damage accumulation is not observed in the undamaged sample. This is potentially due to our low number of cycles; it is possible that the sample was not fatigued enough to initiate the nucleation of microcracks on a large enough scale to affect the modulus of the sample.

Even though the undamaged sample does not behave as expected, the findings from this qualification test validates the use of the damage index to quantify the accumulation of microcracking within a sample. Since all variables are held constant, except for whether or not microcracking is present initially, the clear difference in the rate of damage accumulation between the two samples can be attributed to the amount of microcracking within the sample.

Combination Test Method

Development of Combination Test Method

Although the results from the qualification testing confirmed the validity of using the damage index, a compression-compression test does not emulate the working conditions of the rotor seal closely. The additional shear stress present in the working conditions is critical to the tribological behavior of the rotor seal—a compression-compression fatigue test lacks this shear component.

In order to incorporate the shearing stress, while still being able to fatigue a sample under compressive load, a manual wear rig developed by IDEX was employed (Figure 15). The rig consists of three main components: the sample holder, the load cell, and the manual arm. The sample holder ensures that the pucks stay in contact with the DLC counter surface throughout the test. The load cell is used to measure the load seen by the rotor seal surface, allowing the tightening of the bolts to the correct load. The manual arm is what allows the user to induce the shearing stress, resulting in the cyclic fatiguing of the rotor seal.

Figure 15. The manual wear rig used in the combination test method. The handle on the right side is connected to the test chamber that holds the stator surface and test sample. Compression bolts can be seen running the length of the device. The load cell is on the right side, with a connection running to a digital readout.

Materials & Methods

In order to quantify a material's resistance to the accumulation of microcracks the manual wear rig was used in conjunction with the damage index and visual measurement techniques.

Testing was conducted on a total of six samples: three materials, two samples per material. The three materials tested were chosen because their service life and failure modes are known by IDEX. Since these properties are well documented and the materials are currently in

use, the results from this testing procedure can be used a baseline comparison for future candidate materials.

Each sample needed to be prepared before being tested in the rig. First, .075in was cut off of each sample to create one flat edge on each of the sample pucks; the flat edge ensured that the pucks do not rotate within the sample holder. A strain gauge (Vishay Micro Measurement EA-09-031EC-120) was then adhered to the outer diameter of each puck, in accordance with Vishay's sample preparation techniques for M-Bond 200 adhesive (Figure 16).

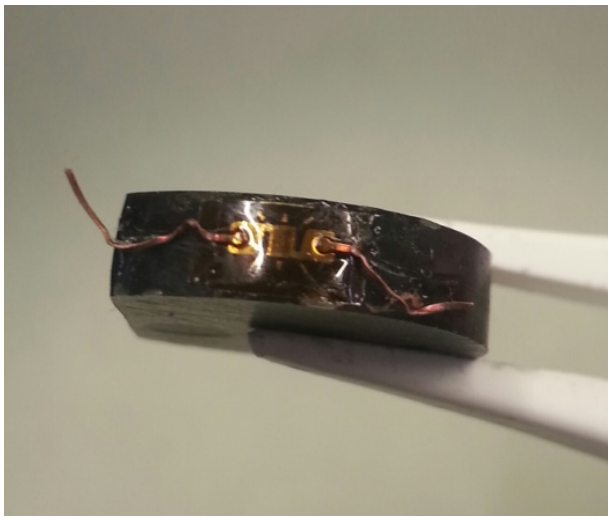

Figure 16. A strain gauge in place on the side of a sample rotor seal. The gold section in the middle is the strain gauge grid, with the copper wire leads attached on either end.

The untested samples were then imaged using scanning electron microscopy and optical microscopy in order to obtain baseline visual data for an unworn state. The SEM used was the FEI Quanta 200, the same used for the failure analysis and with the same low-vac settings. The optical microscope used a polarized light filter for imaging. Because of equipment malfunctions with the SEM, it was necessary to switch to the optical microscope for the second and third wear blocks for all samples.

The samples then underwent compression testing using an Instron 3369 to obtain initial modulus values, in accordance with ASTM standard D0695-10.[9] While inducing a compressive load of 2500, 3000, 3500, 4000, and 4500lbs on the polymer pucks, the resultant strain for each stress state was measured. Once the five loads and corresponding strains, which were obtained

using a Vishay P3 strain recorder, were taken, five modulus values were calculated. The five modulus values were then averaged to obtain the initial modulus of each sample—the two samples for each material were then averaged to obtain one value for each material.

After the initial modulus for all six samples was calculated, the first sample was loaded into the wear rig in a steel sample holder with the rotor seal centered on the stator surface. The rig was then reassembled. To achieve the correct load of 500lbs, the three bolts were tightened one flat at a time in order to maintain equal compression on all sides. Once the load was reached, the rig was clamped to a table surface, and the fatiguing would be conducted by rotating the handle connected to the sample holder 60°, or the distance between two of the rig compression bolts.

Once the sample had been fatigued to 1,000 cycles, it was removed from the rig and imaged again. Following imaging, the sample was loaded back into the Instron to obtain new modulus data, using the same method as previously discussed. This procedure, or wear block, was repeated three times for each sample.

Damage Index Results and Discussion

Once three wear blocks and data collection was complete, the modulus data could be used to calculate the damage index values. By plotting these values, the materials could be compared to each other based on damage accumulated at each wear block (Figure 17).

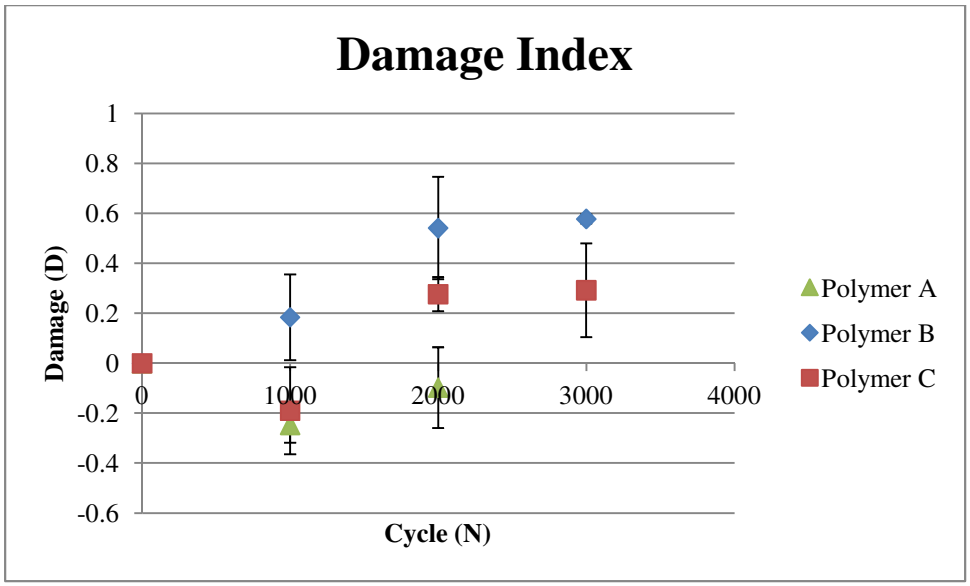

Figure 17: Damage index of the three polymer materials tested.

From these results there are two key points which can be identified. The first is that each of the materials showed a measurable change in the level of damage. As the cycle number increases with each wear block performed, there is an overall change in the modulus of each material, resulting in an increase in damage. This shows that the manual wear rig does create some level of wear that has a definite effect on the damage level of each sample. The second and more important point is that the damage index values for each material are all distinctly different with the progression of the test. This confirms that since all three materials are different, they have distinct damage accumulation rates that can be differentiated from one another. By incorporating this concept in a screening test, when new polymer blends come out, their D_N values could be calculated and compared against the three original materials which will be used as baselines since their real life-cycle performances are already known. This would allow for a quick comparison of the performance of new materials to existing ones, providing some insight on the materials potential for further development.

However, as visible from the data, there is a significant level of variation and uncertainty in the data. Several data points for Polymer A and Polymer C report negative damage, which is neither logical no theoretically possible. As seen from the error bars associated with each data point, there is a large degree of variation for most of the data points. As a result, the ability to draw conclusions regarding data trends is degraded. This can be attributed to the test method

itself. The nature of the manual wear rig incorporates a high degree of variance of the fatiguing conditions. The some of the samples had a small degree of movement due to imperfect machining during sample and rig preparation. To reduce some of this variability, tight tolerances are required in order to ensure that the sample does not shift during the fatigue process so that the same area is fatigued with each wear block. The data collection method could have also contributed to the variance in data. Because the stress and strain data is recorded separately from different sources during the test, there is a chance that they do not correlate to the same exact moment in time. If the strain gauges are not applied in the exact orientation or if they have any residual stresses from the application process, the strain values they report may also affect the data. It should also be noted from Figure 16 that Polymer A does not have a data point for the third wear block at 3000 cycles. This is due to the strain gauge breaking; extreme delicacy must be taken in order to prevent such damage from occurring as use can easily break the lead wires on the strain gauge.

Imaging Results & Discussion

The use of scanning electron microscopy in conjunction with light microscopy provides a visual overview of the damage progression in the samples. This also allowed for a comparison of the life-cycle tested samples provided by IDEX and the samples fatigued by the rig, in terms of the types of damage present. It also provided confirmation of the low level of reliability that the test method has. With the completion of each wear block, the formation of new surface damaged could be noted. Overall, this damage was uncharacteristic of the failure modes seen on the samples examined in the failure analysis, shown in Figure 18. The fact that Polymer B did not show any of this type of damage in the analysis of the life cycle tested rotor seals confirms that the manual wear rig created damage atypical of that seen in actual working conditions. Even with the switch from SEM to optical imaging, the damage progression clearly shows massive amounts of surface scars and deep scratches, as was typical for all sample rotor seals used in this combination test method.

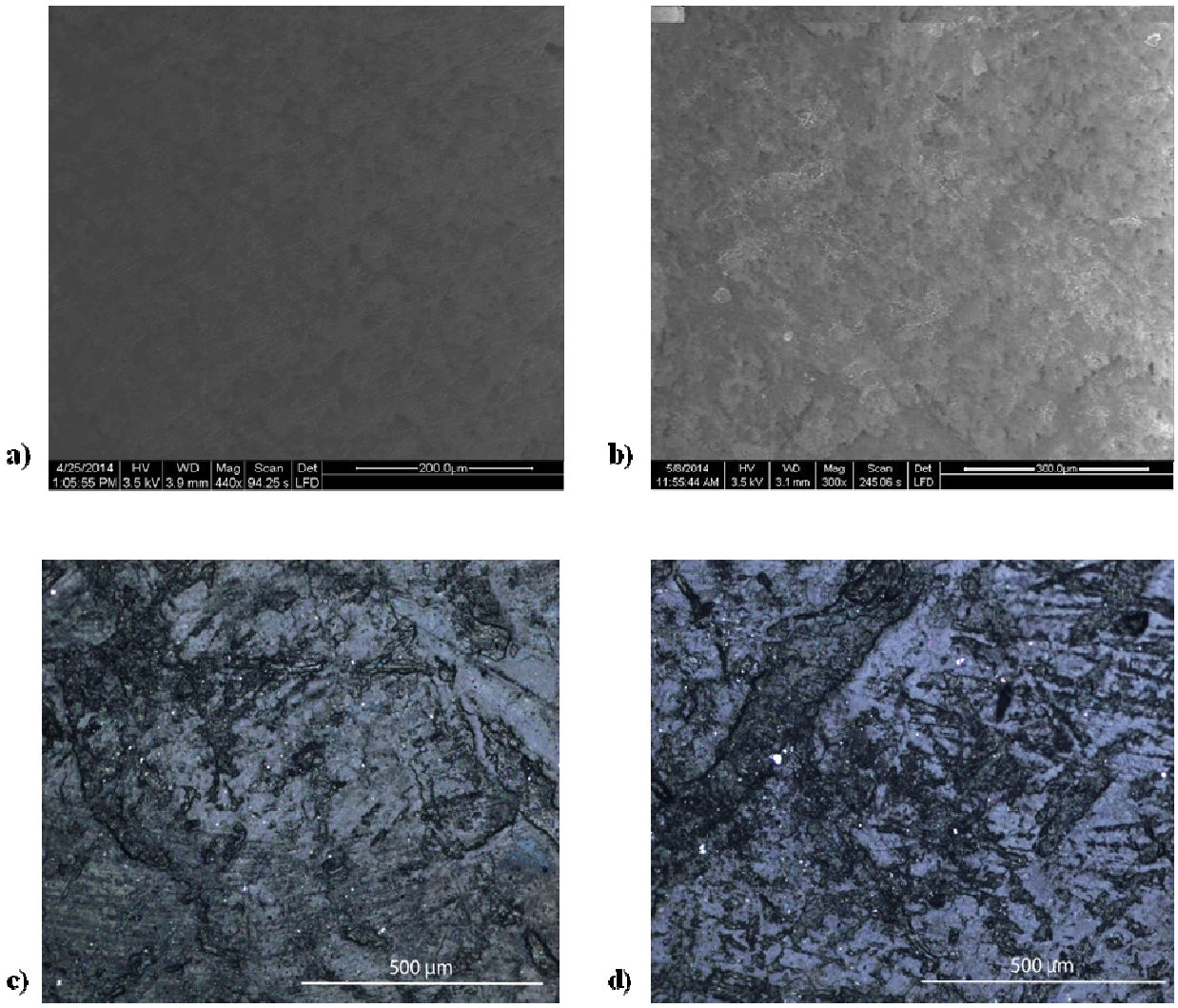

Figure 18: Damage progression in a Polymer B sample used in the combination test method, with images taken at (a) new condition, (b) after the first wear block, (c) after the second wear block, and (d) after the third wear block.

Because of the high level of surface damage, it is nearly impossible to determine whether or not there are any microcracks, spalls, or adhesive wear regions that formed. However, on one sample of Polymer C, a possible spall failure was identified after the third wear block because of its characteristic vertical walls and flat bottom (Figure 19).

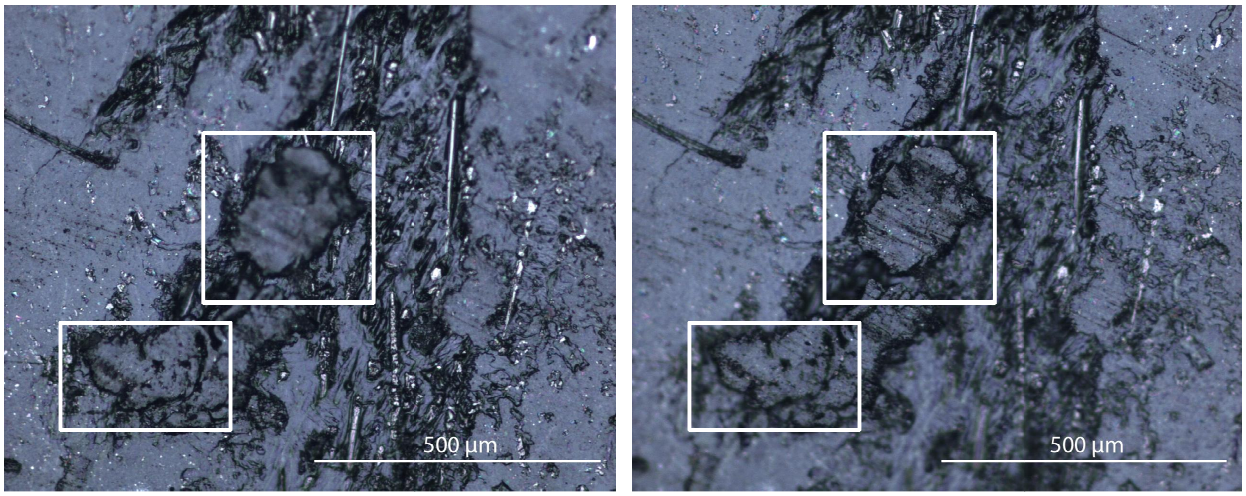

Figure 19: An optical microscope image showing a possible spall divot on the surface of a Polymer C sample after the third wear block. The two focal planes highlight the characteristic vertical walls and flat bottom attributed to spalling failures.

This disparity between the test samples and the rotor seals imaged in the failure analysis can be attributed to the variability of the test. The manual rig is subject to high degrees of human input both in set up and operation. The same stator surface was also used for all rotor seals tested, resulting in the likely addition of third body wear to the system in the form of particles left on the stator surface from previously tested seals. While the stator surface was cleaned after each test, it was most likely not thorough enough to eliminate all contaminants. Comparatively, IDEX's life cycle testing procedure uses an entirely new injector assembly with each new rotor seal in order to eliminate contaminants. The testing also uses automatic machinery, allowing for precise and repeatable movements with constant conditions. The necessary switch from SEM to optical microscopy could have also affected the analysis of the tested samples. Because of the drastic differences in images produced by the two methods, it is possible that microcracking damage could have been missed when using the optical microscope—during failure analysis it was found that large rgions of microcracking could not be seen using the optical microscope. Either way it is likely that the massive amount of surface damage due to 3rd body wear concealing this damage, if it existed.

Moving Forward

There are several possible approaches to testing new materials available to IDEX, each with its own benefits and drawbacks. Considering the resources are available, IDEX has a choice on how they wish to continue forward. In the immediate future, it is recommended that IDEX continues with its current life-cycle testing procedure. This recommendation is made for three reasons:

1) No matter how much time and money is put into emulating the working conditions of the rotor seal, the most accurate representation will always be to use an actual injector assembly.
2) The current development rate of materials is so slow that the costs associated with a rejection in the life-cycle testing are spread out over enough time that they can be absorbed by IDEX without being too detrimental.
3) The results of full life-cycle testing have been confirmed by IDEX over the years and are considered accurate. It is also done in order to certify all materials for sale as rotor seals.

However, should IDEX choose to continue development of a viable preliminary screening test for candidate materials, it is recommended that a compression-compression fatigue test from which the damage index is calculated be investigated further. This is due to its use in the qualification test which shows a clear difference in a material with and without microcracking present. With this initial testing and data analysis concept in place, its use for screening candidate materials could be confirmed with further testing that uses larger sample sizes and a higher number of cycles. As this test only accounts for microcracking as a single mode of failure, it should be combined with a wear test accordance with ASTM standard D3702 in order to more accurately predict the tribological behavior of candidate materials.[11]

Another possibility is the use of modeling software. Although the software is expensive and the modeling of tribological properties of composites with randomly oriented fiber reinforcement is highly complex and difficult, once a method is developed, it can be run as many times as necessary with small parameter changes being made easily. This would result in much lower costs, as it does not require any material purchased, physical parts be manufactured or additional machinery, and the time spent is cut from months to days.

References

1. Frederic Gerber, Markus Krummen, Heiko Potgeter, Alfons Roth, Christoph Siffrin, Christoph Spoendlin, Practical aspects of fast reversed-phase high-performance liquid chromatography using 3µm particle packed columns and monolithic columns in pharmaceutical development and production working under current good manufacturing practice, Journal of Chromatography A, Volume 1036, Issue 2, 21 May 2004, Pages 127-133, http://www.sciencedirect.com/science/article/pii/S0021967304003139.

2. "Thermoplastic PEEK Review." Engineer's Edge, n.d. Web. 5 Dec. 2013. http://www.engineersedge.com/plastic/plastic_material/polyetheretherketone-peek-plastic.htm.

3. Advanced Thermoplastics, *Engineered Materials Handbook Desk Edition*, ASM International, 1995, p. 206–249

4. D.A. Scola, Polyimide Resins, *Composites*, Vol 21, *ASM Handbook*, ASM International, 2001, p. 105–119

5.Properties and Performance of Polymer-Matrix Composites, *Composites*, Vol 21, *ASM Handbook*, ASM International, 2001, p 803–837

6. R.L. Widner, Failures of Rolling-Element Bearings, *Failure Analysis and Prevention*, Vol 11, *ASM Handbook*, ASM International, 1986, p 490–513

7. Mallick, P. K. "Fracture Behavior and Damage Tolerance." *Fiber-reinforced Composites: Materials, Manufacturing, and Design*. Third ed. Boca Raton, FL: CRC, 2008. 345+. Print.

8. Avanzini, A., G. Donzella, D. Gallina, S. Pandini, and C. Petrogalli. "Fatigue Behavior and Cyclic Damage of Peek Short Fiber Reinforced Composites."*Composites Part B: Engineering* 45.1 (2013): 397-406. Web. Winter 2014.

9. ASTM Standard D0695, 1996 (2010), "Standard Test Method for Compressive Properties of Rigid Plastics," ASTM International, West Conshohocken, PA, 1996, DOI: 10.1520/D0695-96R10, www.astm.org

10. ASTM Standard D7791, (2012), "Standard Test Method for Uniaxial Fatigue Properties of Plastics," ASTM International, West Conshohocken, PA, 1996, DOI: 10.1520/D7791-12, www.astm.org

11. ASTM Standard D3702, 1994 (2009), "Standard Test Method for Wear Rate and Coefficient of Friction of Materials in Self-Lubricated Rubbing Contact Using a Thrust Washer Testing Machine," ASTM International, West Conshohocken, PA, 1994, DOI: 10.1520/D3702-94R09, www.astm.org

Appendix A

Data Preparation- Qualification Testing

In order to obtain modulus data, on a per cycle basis, each cycle of load-strain data outputted from the Instron must first be isolated. To accomplish this standard data smoothing techniques were used on the load data.

1) Apply a 3 median smooth
2) Apply a 3 median smooth again
3) Apply a Hanning smooth
4) Apply a skip-mean smooth

Once the load data is smoothed, the correct part of the stress-strain curve must be isolated. The part of the stress-strain curve which is used in calculating the elastic modulus is the portion in which load and strain are increasing. In order to isolate this region of the curve, for each cycle, excel was used. The following steps are first presented in terms of the syntax used in excel, and then each step is interpreted verbally.

1) Put load data in column A, strain data in column B
2) In column C, apply "=A1/.33"
3) In column D, apply "=IF(AND(A1>4000,A1<4400),(C1/(B1*(10^-6)*-1)),"")"
4) In column E, apply "=IF(AND(D1="",D2<>""),1,"")"
5) In column F, apply "=IF(E1<>"",SUM($E$1:E1),"")"
6) In column G, ascend from 0 to the last number in column E, counting even numbers only
7) In column H, apply "=(INDEX($D$1:DD,MATCH($G$1,$F:$F,0),1))"
8) In column I, apply "=(INDEX($D$1:DD,MATCH($G$1,$F:$F,0)+1,1))"
9) In column J, apply "=(INDEX($D$1:DD,MATCH($G$1,$F:$F,0)+2,1))"
10) In column K, apply "=(INDEX($D$1:DD,MATCH($G$1,$F:$F,0)+3,1))"
11) Repeat until column R contains "=(INDEX($D$1:DD,MATCH($G$1,$F:$F,0)+10,1))"
12) In column S, apply "=AVERAGE(H1:R1)"
13) In column T, apply "=1-(S1/$S$1)", this is now the damage index value
14) Graph column T (damage index) vs column G (cycle number)

Note on .33: this is the sample area; adjust accordingly

Note on A1>4000,A1<4400: this is the range of load values which are known to fall within the region of the stress-strain curve which is wished to be isolated; adjust accordingly

Note on counting even numbers only: since load values from both the loading and unloading portions of the test will satisfy the "if statement" in step #3, either only the odd or even number outputted in column F should be counted. By counting only the even numbers in this study the unloading portion of the stress-strain curve is omitted; depending on the data set however, it might be necessary to count only the odd numbers; adjust accordingly.

1) Sheet set-up
2) Obtain stress values
3) Obtain modulus values for given load interval

4) Create a “placemarker” (1) when at the beginning of a new half-cycle (both unloading and loading regions currently counted as a separate cycle)
5) Running sum of placemarkers, effectively translating them to half-cycle numbers
6) Set-up which half-cycles are counted, only counting the loading portion
7) Match half-cycle number in step #6 to half-cycle number in step #5, and return the corresponding modulus value
8) Returns the next modulus value down from step #7
9) Returns the next modulus value down from step #8
10) Returns the next modulus value down from step #9
11) Returns the next moduli value down from step #10
12) Averages the 10 moduli values from steps #7-#11
13) Obtain damage index values
14) Graph